Physica Scripta

PAPER

Theoretical investigation of the elastic scattering of $e^{\pm}$ by the ions of nitrogen isonuclear series

IOP Publishing Physica Scripta
Phys. Scr. 95 (2020) 085403 (11pp) https://doi.org/10.1088/1402-4896/ab9cfb

Theoretical investigation of the elastic scattering of $e^{\pm}$ by the ions of nitrogen isonuclear series

M Shorifuddoza[1,2], Mahmudul H Khandker[2], A K F Haque[2,3,4], Hiroshi Watabe[5] and M Alfaz Uddin[1,2]

[1] Department of Physics, Pabna University of Science and Technology, Pabna-6600, Bangladesh
[2] Atomic and Molecular Physics Lab, Department of Physics, University of Rajshahi, Rajshahi-6205, Bangladesh
[3] Nanosciences African Network (NANOAFNET), Materials Research Group (MRG), iThemba LABS-National Research Foundation (NRF), 1 Old Faure Road, 7129, PO Box 722, Somerset West, Western Cape Province, South Africa
[4] UNESCO-UNISA Africa Chair in Nanosciences/Nanotechnology Laboratories, College of Graduate Studies, University of South Africa (UNISA), Muckleneuk Ridge, PO Box 392, Pretoria, South Africa
[5] Division of Radiation Protection and Safety Control, Cyclotron and Radioisotope Center, Tohoku University, 6-3 Aoba, Aramaki, Aoba, Sendai 980-8578 Japan

E-mail: fhaque@ru.ac.bd

Received 5 March 2020, revised 2 June 2020
Accepted for publication 15 June 2020
Published 2 July 2020

Abstract

This work reports on differential, integrated and momentum transfer cross sections for the elastic scattering of electrons and positrons off the ions of nitrogen isonuclear series (N^{+} - N^{7+}) over the energy range 1–500 eV. Calculations of these observable quantities involve the solution of Dirac relativistic wave equation employing a pure Coulomb potential and a short range potential. The latter comprises static, exchange, polarization and absorption potentials. Effects of these individual potentials on angular distribution of elastically scattered electrons are investigated throughout this ionic series. Differential cross sections for electron and positron scattering are compared with each other to demonstrate the difference of their collision dynamics. A satisfactory agreement between our predictions and other available data, experimental and theoretical, is observed.

Keywords: electron and positron-ion scattering, nitrogen ions, modifed Coulomb field, Dirac partial wave analysis, isonuclear series

(Some figures may appear in colour only in the online journal)

1. Introduction

Elastic scattering of electrons and positrons from ions is an important fundamental process to probe the atomic structure of matter and transport of these projectiles through the ionized matter is used to simulate various physical processes. Electron-ion collision data are required to understand the behavior of plasmas occurring in many research and technical fields such as artificial and astrophysical plasmas, fusion energy research, semiconductor lithography, the upper atmosphere and ionosphere, discharge gases, x-ray lasers, radiobiology, etc [1–5]. On the other hand, understanding positron-ion collisions is one of the possible key to place constraints on the origin of positrons by determining whether the observed spatial distribution of positron emission in our Galaxy reflects the spatial distribution of positron sources [6]. The presence of nitrogen ions in the magnetosphere of Earth and Saturn [7, 8], in the atmosphere [9] and their applications in nitrogen ion laser [10], nitrogen ion implantation [11] and nitrogen ion microscopy [12] makes these ions more relevant to study.

Although the study of the scattering of electron and positron from neutral atoms have been extensively done, the

same from ions are not many. Particularly, works on positron-ion scattering are very limited. As the positron is an anti-matter, the interaction of matter and antimatter in positron-ion scattering might unravel new physics and open up possibilities for applications like electron-ion scattering. The investigation of electron scattering from gases began to be active area of research since ground-breaking works of Ramsauer [13], Townend and Bailey in 1920s [14]. The first positron-atom scattering experiment was performed in the early 1970s by Costello *et al* [15]. The 1980s have seen a burgeoning growth of measurements of scattering observables with the developments of intense positron beam and improvements of measuring techniques.

The advent of modern accelerators, efficient detectors and recent opportunity of getting multiply charged ion sources have provided the chance to measure the observables of electron-ion collisions. Williams *et al*. [16] published the measurement on differential cross sections (DCSs) for the elastic collisions of electron by N^{+}, N^{2+} and N^{3+} at 10eV. DCS for the 2s $\rightarrow$ 2p excitation of N^{4+} at collision energy 50 eV is reported by Huber *et al* [17].

Literature lacks in extensive studies of electron-ion scattering. Few theoretical works have been reported for e^{-}– N^{q+} scattering. Szydlik *et al*[18] computed phase shifts for the elastic collisions of electrons from positive ions of nitrogen using independent particle model (IPM) potentials. Employing model- and pseudopotential and quantum defect methods, Shepherd and Dickinson [19] have calculated the DCSs for the elastic scattering of electrons from the ions Na^{+}, Cs^{+}, Mg^{2+}, N^{3+} and Ar^{8+}. They have used the model potential of McCarroll and Valiron [20] for N^{3+} ion. Greenwood and Williams [21] reported on momentum transfer cross sections for the elastic collisions of electron by N^{q+} at 27.2 eV using Rutherford scattering formula and partial wave analysis. As far as our knowledge goes, no other experiment and theoretical studies have been performed for this scattering system. Due to the difficulties in performing positron-ion scattering experiment [22], experimental data on positron-ion scattering are very rare in literature.

Despite the above mentioned importance, works, theoretical or experimental, on the scattering of electron and positron from nitrogen ions are inadequate in literature. Hence the investigation of $e^{\pm}$- N^{q+} collision dynamics might be an interesting and useful study. Motivated by this research drive, present work undertakes the theoretical investigation of the elastic collisions of electrons and positrons from the positive ions of nitrogen isonuclear series in an objective to study the charge and energy dependence of various cross sections. The scattering of primary electrons by a fully stripped ion is dominated by the asymptotic Coulomb potential and so governed by the Rutherford scattering formula for the angular differential cross sections. When the bare nucleus is replaced by a partially dressed ion, interference structure is observed particularly at large scattering angles. This interference structure is a sensitive probe of the interactions of the bound electrons and incident projectiles (electron and positron). To elucidate this structure in DCS, long range Coulomb potential is supplemented by a short range potential arising due to the interaction of projectile with the spatial charge distribution of bound electrons and nuclear protons. This combined recipe, termed as modified Coulomb potential, is used in this work to calculate observable quantities for $e^{\pm}$-N^{q+} elastic scattering in the framework Dirac partial wave analysis.

A complex optical potential model (OPM), comprising both real and imaginary parts, is used to serve the function of short range potential. The real part consists of static, exchange and polarization potentials. The main contribution to the OPM comes from the electrostatic potential. Under static field approximation, this potential is completely generated by nuclear [23] and electronic [24] charge distributions. Two major effects are needed to include with the real part of the potential to describe the scattering phenomenon adequately. One is the rearrangement collision between primary and bound electrons and another is the distortion of electron cloud by the electric field of the projectile. An approximate local potential given by Furness and McCarthy [25] is used to deal this non-local exchange interaction and Buckinghum polarization potential is used to describe the effects of distortion of the electron cloud. Rearrangement collision is omitted in case of positron scattering due to the distinguishability of positron and dressing electrons. Above the first inelastic threshold, the real potential is not ample enough to describe the scattering phenomenon exclusively. Above this threshold, inelastic channels become open and cause a depletion of elastically scattered electrons due to loss of incident flux. This depletion is described by a semi-relativistic absorptive potential [26].

In this work, a modified Coulomb potential, which includes a complex short range and a long range Coulomb potential, is employed within the framework of Dirac partial wave analysis to calculate DCS for the elastic collisions of incoming electrons and positrons and integrated elastic cross section (IECS) and momentum transfer cross section (MTCS) for electrons from the aforesaid ions of nitrogen isonuclear series over the energy range 1 eV–500 eV using ELSEPA code [26]. We compare our results with the available experimental data [16] and other theoretical predictions [18–20].

2. Theory

2.1. Interaction potential

The modified Coulomb potential for the scattering of electron and positron by a target ion of charge qe is given as

$$V(r) = V_{coul}(r) + V_{sr}(r) = \frac{zqe^2}{r} + V_{sr}(r). \qquad (1)$$

Here, $z = -1$ for electron and $z = 1$ for positron. $V_{coul}(r)$ is the Coulomb potential, which arises due to Coulomb interaction between the charged projectile and target ion and $V_{sr}(r)$ is the short range potential arises due to the interaction of scattering electrons and positrons with the screening electrons and nuclear protons. The short range optical potential is given as [26]

$$V_{sr}(r) = V_{st}(r) + V_{ex}(r) + V_{cp}(r) - iW_{abs}(r). \qquad (2)$$

Here, V_{st}, V_{ex}, V_{cp} and W_{abs} are static, exchange, correlation-polarization and absorption potentials, respectively. The quantity ze^2q/r is subtracted from $V_{sr}(r)$ in equation (2) to make it a short range potential in and around the matching distance.

Considering the electron cloud of the target ion as a frozen distribution of charge, static potential is generated by the electrostatic interaction of the projectile with the screening electrons and nuclear protons and is given as

$$V_{st}(r) = ze[\phi_n(r) + \phi_e(r)], \tag{3}$$

where ze is the charge of the projectile. ϕ_e and ϕ_n are the contributions of the atomic electron cloud and nuclear protons to the electrostatic potential, which can be written as

$$\phi_n(r) = e\int d\mathbf{r}'\frac{\varrho_n(r')}{|\mathbf{r}-\mathbf{r}'|} \tag{4}$$

and

$$\phi_e(r) = -e\int d\mathbf{r}'\frac{\varrho_e(r')}{|\mathbf{r}-\mathbf{r}'|}. \tag{5}$$

Here, ϱ_n and ϱ_e are the proton and electron densities of the target ion. Both these density functions are normalized by the following equation

$$\int \varrho(r)4\pi r^2 dr = Q, \tag{6}$$

For ϱ_e, $Q = Z - q$, the number of screening electrons of the target ion and for ϱ_n, $Q = Z$ with Z being the atomic number of the target. In this work, following two parameter Fermi distribution [23] is used to provide the proton density

$$\varrho_n = \frac{\varrho_0}{1 + e^{(r-R_n)/a}} \tag{7}$$

where, the nuclear size parameter $R_n = 2.58$ fm and the surface diffuseness parameter $a = 0.546$ fm for the ^{14}N nucleus. ϱ_0 is normalization constant according to (6). Dirac-Fock electron density generated by Desclaux code [24] is used for ϱ_e in our investigation.

Exchange interaction between the projectile electron and screening electrons arising due to the Pauli's exclusion principle is a unique feature of electron scattering. This interaction is non-local by nature and leads to a set of coupled integro-differential equations. Solutions of these equations are Considerably complicated. It is thus desirable to have an approximation to this non-local potential. A semi-classical local exchange potential of Furness and McCarthy [25] of the following form is used in our present work

$$V_{ex}(r) = \frac{1}{2}[E_i - V_{st}(r)] - \frac{1}{2}\{[E_i - V_{st}(r)]^2 + 4\pi a_0 e^4 \varrho_e(r)\}^{1/2}. \tag{8}$$

Here, E_i and a_0 are the incident electron energy and the Bohr radius, respectively. Besides the easy numerical solution, this approximate potential can provide easy and accurate solution to the scattering problem. In case of positron scattering, this potential is omitted due to the distinguishability of the positron and target electrons.

As the projectile approaches the target, its electric field causes distortion of the target's electron cloud and hence a dipole moment is induced in the ion. This induced dipole attracts back the projectile. This attraction can be described by the Buckinghum polarization potential

$$V_{pol}(r) = -\frac{\alpha_d e^2}{2(r^2 + d^2)^2}. \tag{9}$$

Here, $\alpha_d = 1.10 \times 10^{-24}$ cm^3 is the dipole polarizability of nitrogen atom. d, a phenomenological cut off parameter, is introduced to avoid singularity of this potential at $r = 0$ and can be expressed as [27]

$$d^4 = \frac{1}{2}\alpha_d a_0 (Z - q)^{-1/3} b^2, \tag{10}$$

where b is an adjustable energy dependent parameter. The parameter d in the above equation fits the $V_{pol}(r)$ for the corresponding ion through the term $(Z - q)$ that represents the number of core electrons. In the asymptotic region $(r \gg d)$, V_{pol} varies as r^{-4} and so is negligibly small in comparison to the strong Coulomb repulsion (for $q > 0$), thereby having almost negligible effect on the cross sections. Since atomic electrons do not react instantaneously to external electric fields, the magnitude of the polarization effects decreases as the projectile energy increases. Considering this fact, Seltzer [28] suggested the following empirical formula:

$$b^2 = \max\{(E - 50\,eV)/(16\,eV), 1\}. \tag{11}$$

When energy of the projectile electron is greater than the first excitation threshold, the inelastic channels become open and causes a depletion of elastically scattered electrons. A negative imaginary potential $-iW_{abs}$ is needed to describe this effect. Under local density approximation, the absorption probability of an electron of local kinetic energy E_l interacting with atomic electron cloud of density ϱ_e at a distance r is given as [26, 28, 29]

$$(2/\hbar)W_{abs}(r) = A_{abs}\frac{v_{nl}}{v_{rl}}[\varrho_e(r)v_{nl}\sigma_{bc}(E_l, \varrho_e, \Delta)], \tag{12}$$

where, the non-relativistic velocity, $v_{nl} = \sqrt{\frac{2E_l}{m_e}}$, relativistic velocity [26],

$$v_{rl} = c\frac{\sqrt{E_l(E_l + 2m_e c^2)}}{(E_l + m_e c^2)}, \tag{13}$$

$\sigma_{bc}(E_l, \varrho_e, \Delta)$ is the one electron cross section [28] for inelastic scattering involving energy transfer greater than the energy gap Δ, which is adopted as

$$\Delta = \begin{cases} \epsilon_1 & \text{for electron,} \\ \max\{I - 6.8\,\text{eV}, 0\} & \text{for positron,} \end{cases} \tag{14}$$

where, ϵ_1 is first excitation energy and I is the ionization potential of nitrogen atom and 6.8 eV is the positronium binding energy. The local kinetic energy is given by

$$E_l(r) = \begin{cases} E_i - V_{st}(r) - V_{ex}(r) & \text{for electron} \\ \max\{E_i - V_{st}(r), 0\} & \text{for positron.} \end{cases} \tag{15}$$

The semi-relativistic absorptive potential can now be written as [26]

$$W_{abs}(r) = \sqrt{\frac{2(E_l + m_e c^2)^2}{m_e c^2 (E_l + 2m_e c^2)}} \times A_{abs} \frac{\hbar}{2} [\varrho_e(r) v_{nl} \sigma_{bc}(E_l, \varrho_e, \Delta)]. \quad (16)$$

The strength of the potential is determined by the adjustable parameter A_{abs} that depends on the combination of projectile and target. In this work, the value of this parameter is taken as 2.2.

2.2. Partial wave analysis

The Dirac equation for the modified Coulomb potential in equation (1) admits spherical wave solutions. After appropriate normalization of the spherical waves, the asymptotic form of the upper component radial function can be expressed as

$$P_{E\kappa}(r) \sim \sin\left(kr - \ell\frac{\pi}{2} - \eta \ln 2kr + \delta_\kappa\right). \quad (17)$$

Here $k = (1/\hbar c)\sqrt{E_i(E_i + 2m_e c^2)}$ is the projectile's relativistic wave number, $\kappa = (\ell - j)(2j + 1)$ is the relativistic quantum number with j and ℓ being the total and orbital angular momentum quantum numbers and $\eta = \frac{qe^2 m_e}{\hbar k}$ is the Sommerfeld parameter for Coulomb tail. δ_κ is the global phase shift that represents the asymptotic behavior of Dirac spherical wave. It is expressed as [30]

$$\delta_\kappa = \Delta_\kappa + \hat{\delta}_\kappa, \quad (18)$$

where Δ_κ is the Coulomb phase shift of the potential tail and $\hat{\delta}_\kappa$ is the inner phase shift caused by the short range potential. Coulomb phase shift Δ_κ can be found by solving Dirac equation for the Coulomb part ($V_{coul} = zqe^2/r$) of the potential in equation (1) as [31]

$$\Delta_\kappa = \arg[\zeta(E_i + 2m_e c^2) - i(\kappa + \lambda)c\hbar k] - (\lambda - \ell - 1)\frac{\pi}{2} + \arg\Gamma(\lambda + i\eta) - S_{\zeta,\kappa}\pi, \quad (19)$$

where, $\zeta = \frac{qe^2}{\hbar c}$, $\lambda = \sqrt{\kappa^2 - \zeta^2}$, and $S_{\zeta,\kappa} = 1$ if $\zeta < 0$ and $\kappa < 0$, and $= 0$ otherwise. The direct, $f^{(C)}(\theta)$, and spin-flip, $g^{(C)}(\theta)$ scattering amplitudes for scattering of electrons and positrons by $V_{coul}(r)$ with $q = Z$ can now be calculated using the partial-wave expansions as

$$f^{(C)}(\theta) = \frac{1}{2ik}\sum_{\ell=0}^{\infty}\{(\ell + 1)[\exp(2i\Delta_{-\ell-1}) - 1] + \ell[\exp(2i\Delta_\ell) - 1]\}P_\ell(\cos\theta) \quad (20)$$

and

$$g^{(C)}(\theta) = \frac{1}{2ik}\sum_{\ell=0}^{\infty}\{\exp(2i\Delta_\ell) - \exp(2i\Delta_{-\ell-1})\}P_\ell^1(\cos\theta). \quad (21)$$

Inner phase shifts $\hat{\delta}_\kappa$, caused by short range potential, are calculated by integrating radial equations from $r = 0$ to a certain distance r_m beyond which the field is purely Coulombian. The normalized upper component radial function can be expressed as a linear combination of regular, $f^u_{E\kappa}(r)$ and irregular, $g^u_{E\kappa}(r)$ Dirac-Coulomb functions by the following expression

$$P_{E\kappa}(r) = \cos\hat{\delta}_\kappa f^{(u)}_{E\kappa}(r) + \sin\hat{\delta}_\kappa g^{(u)}_{E\kappa}(r). \quad (22)$$

The phase shift $\hat{\delta}_\kappa$ can now be determined by matching log derivative of outer analytical form to the inner numerical solution at r_m, requiring continuity of the radial function $P_{E\kappa}(r)$ and its derivative. This method gives

$$\exp(2i\hat{\delta}_\kappa) = \frac{D_{out}[f^{(u)}_{E\kappa}(r_m) + ig^{(u)}_{E\kappa}(r_m)] - [(f^{(u)}_{E\kappa})'(r_m) + i(g^{(u)}_{E\kappa})'(r_m)]}{[(f^{(u)}_{E\kappa})'(r_m) - i(g^{(u)}_{E\kappa})'(r_m)] - D_{out}[f^{(u)}_{E\kappa}(r_m) - ig^{(u)}_{E\kappa}(r_m)]}, \quad (23)$$

where the primes specify the derivatives with respect to r and D_{out}, the logarithmic derivative of the outgoing numerical radial function at the matching point. The phase shift $\hat{\delta}_\kappa$ is complex as the short range potential V_{sr} is taken as complex in the present work. The scattering amplitudes $f_{sr}(\theta)$ and $g_{sr}(\theta)$, for the short range potential, are given as

$$f_{sr}(\theta) = \frac{1}{2ik}\sum_{\ell=0}^{\infty}\{(\ell + 1)\exp(2i\Delta_{-\ell-1})[\exp(2i\hat{\delta}_{-\ell-1}) - 1] + \ell\ \exp(2i\Delta_\ell)[\exp(2i\hat{\delta}_\ell) - 1]\}P_\ell(\cos\theta) \quad (24)$$

and

$$g_{sr}(\theta) = \frac{1}{2ik}\sum_{l=0}^{\infty}\{\exp(2i\Delta_\ell)[\exp(2i\hat{\delta}_\ell) - 1] - \exp(2i\Delta_{-\ell-1})[\exp(2i\hat{\delta}_{-\ell-1}) - 1]\}P_l^1(\cos\theta). \quad (25)$$

The direct and spin flip scattering amplitudes, $f(\theta)$ and $g(\theta)$ for the scattering of electrons and positrons can be written as

$$f(\theta) = f^{sr}(\theta) + f^C(\theta), \quad g(\theta) = g^{sr}(\theta) + g^C(\theta). \quad (26)$$

In calculating the V_{st}, and phase shifts, the integration is done from $r = 0$ to r_m, a distance greater than the range of the short range potential. As a result, the distributed form of the charge of the nucleus does affect the V_{st} and the solution of the Dirac equation and so the scattering observables. The differential, integrated elastic and momentum transfer cross sections are calculated in our work using the following formulas

$$\frac{d\sigma}{d\Omega} = |f(\theta)|^2 + |g(\theta)|^2, \quad (27)$$

$$\sigma_{el} = \int\frac{d\sigma}{d\Omega}d\Omega = 2\pi\int_0^\pi (|f(\theta)|^2 + |g(\theta)|^2)\sin(\theta)d\theta, \quad (28)$$

and

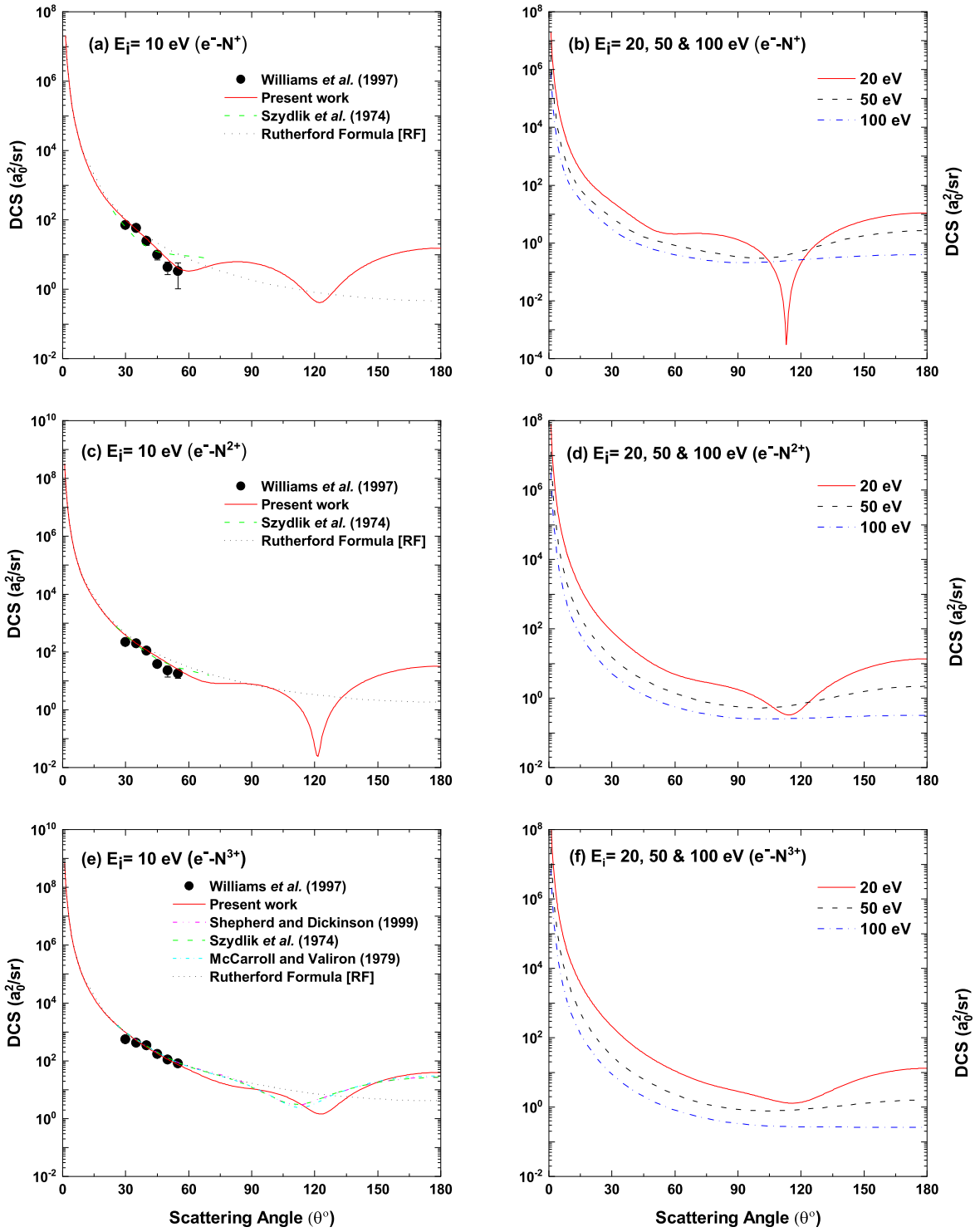

Figure 1. DCS (a_0^2/sr) for the elastic collisions of electrons from (a) and (b) N^+; (c) and (d) N^{2+}; (e) and (f) N^{3+} at E_i = 10, 20, 50 & 100 eV. Theoretical: Szydlik *et al* [18], Shepherd and Dickinson [19] and McCarroll and Valiron [20]. Experimental: Williams *et al* [16].

$$\sigma_m = 2\pi \int_0^{\pi} (1 - \cos\theta)(|f(\theta)|^2 + |g(\theta)|^2)\sin(\theta)d\theta. \quad (29)$$

In case of totally stripped nitrogen, DCS can be written as

$$\frac{d\sigma}{d\Omega} = |f^C(\theta)|^2 + |g^C(\theta)|^2. \quad (30)$$

The partial-wave series converge very slowly for the small angle elastic scattering by ions. There is scope for 25 000 partial waves. Angular momentum is increased up to a certain maximum for which the absolute value of the phase shift is less than 10^{-9}. At this point partial wave expressions for $f(\theta)$ and $g(\theta)$ converge to the required accuracy (usually more than six decimal places) for all angles. In the calculations of scattering amplitudes and cross sections, scattering angles larger than 1° are considered to avoid the divergence [26]. CGS Gaussian units are used to express equations in the manuscript unless otherwise

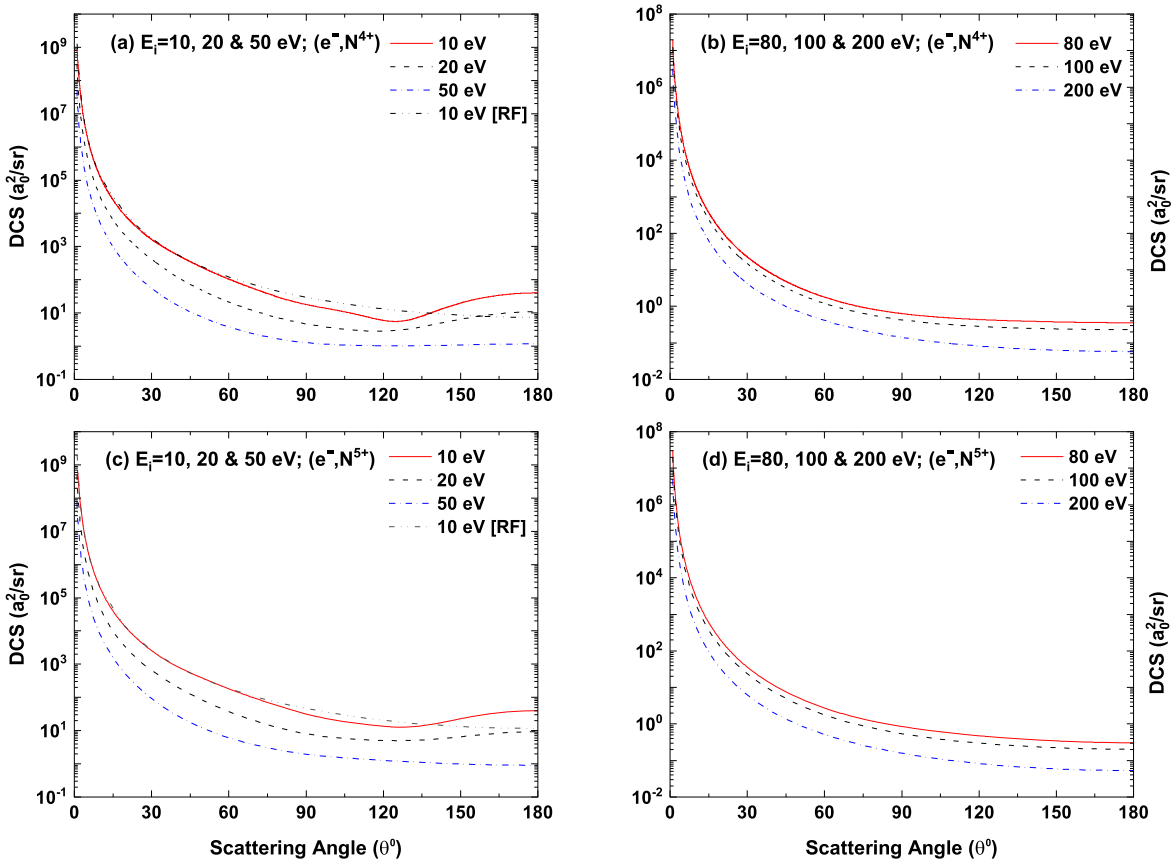

Figure 2. DCS (a_0^2/sr) for the elastic collisions of electrons from (a) and (b) N^{4+}; (c) and (d) N^{5+} at E_i = 10, 20, 50, 80, 100 & 200 eV. Theoretical: Present work (solid, dash, dash dot and dash dot dot lines).

specified and atomic units are used in the calculations in the FORTRAN code [26]. Numerical Dirac-Fock electron density [24], generated from the numerical relativistic wavefuntion of the target, is used in our work.

3. Results and discussions

This work presents the calculations of DCS, IECS and MTCS for the elastic scattering of electrons and positrons from the ions of nitrogen isonuclear series in the energy range 1 eV–500 eV. Calculated results are compared with the experimental measurements of Williams *et al* [16] and the theoretical calculations of Szydlik *et al* [18], Shepherd and Dickinson [19] and McCarroll and Valiron [20].

In figure 1(a), our DCS calculations for singly charged ion N^+ at 10 eV are compared with the experimental data [16], Rutherford scattering and the IPM calculations of Szydlik [18]. Our predictions show good agreement with the experimental data along with the reproduction of interference minimum at ∼55°. IPM calculations fails to reproduce this interference dip. Our method closely predicts the observed deviation of experimental data from Rutherford behavior. Comparatively less strong interference structure for doubly charged ion N^{2+} is observed in the experimental DCS [16]. Our model quite reasonably reproduces this observation. In figure 1(e), our and other [18–20] calculations reasonably agree with the experimental data [16]. Our calculations differ from those of Shepherd and Dickinson [19] and McCarroll and Valiron [20] by predicting a minimum at ∼125°, which is comparatively more dip and shifted towards right.

From figures 1(a), (c) and (e), we see the dwindling of interference structure with the increase of charge states in consistence with the experimental data. Interference in DCS occurs due to the coherent interference of the waves scattered from the short range and Coulomb potentials. This interference is observed remarkably for the scattering of low energy electrons from the ions of lower degrees of ionicities, particularly for backward scattering that reflects the penetration of the incoming electrons into the core of the ion. Low electron velocity causes enhanced electron-electron correlation and thereby making the short range potential contribute significantly to interference phenomenon. Increasing charge states decreases the screening of the target. This in turn causes the Coulomb interaction to dominate over the scattering. As a result, Rutherford like behavior starts to become prominent following the gradual fading of interference structure with the rise of ionicity. From figures 1(a)–(f), it is also observed that at a particular charge state, interference structure fades away with the increase of energy. This is due to the incoherent interference of large number of angular momentum states.

In figures 2 and 3, we present DCS for N^{4+}, N^{5+}, N^{6+} and N^{7+} at energies 10, 20, 50, 80, 100 and 200 eV. Coulomb domination is prominent for most of the ionic members of

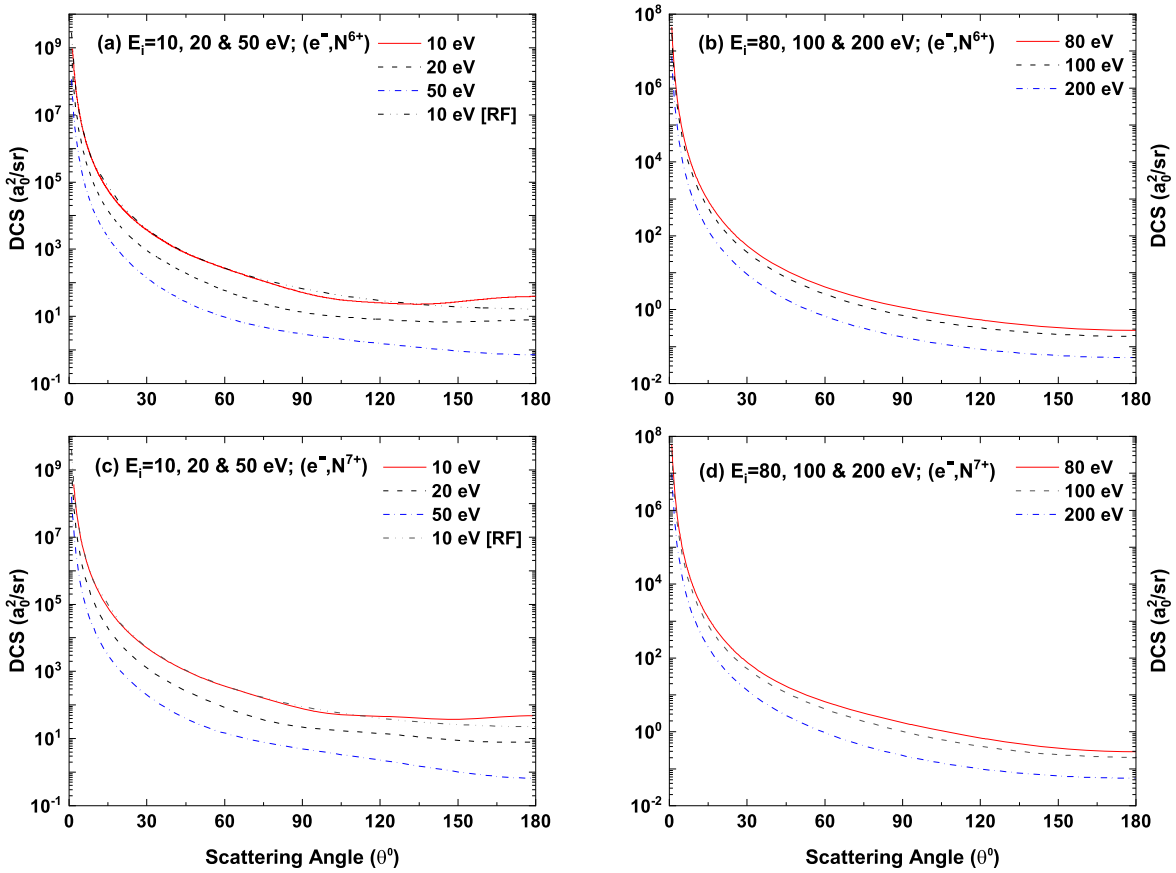

Figure 3. Same as figure 2 from (a) and (b) N^{6+}; (c) and (d) N^{7+}. Theoretical: Present work (solid, dash, dash dot and dash dot dot lines).

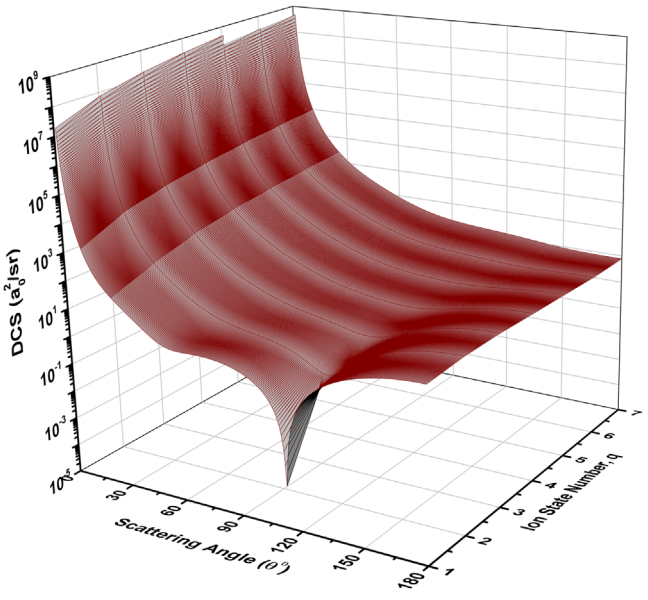

Figure 4. Variation of DCS (a_0^2/sr) with the degree of ionicity at $E_i = 20$ eV.

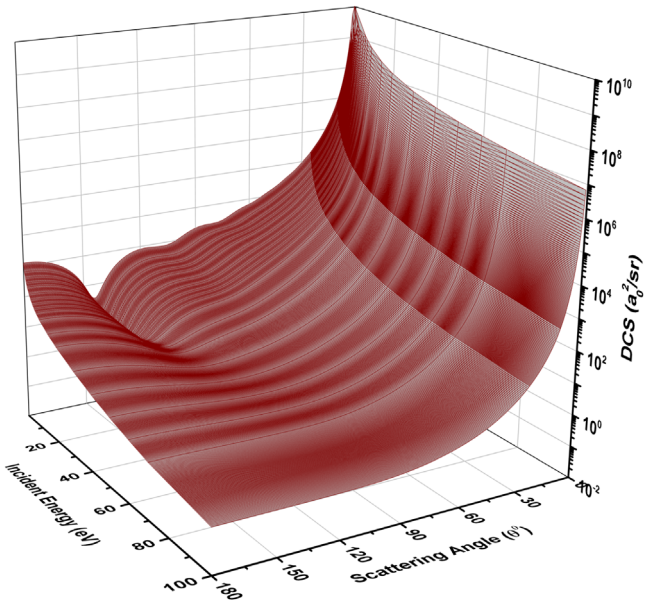

Figure 5. Variation of DCS (a_0^2/sr) with the incident electron energy for N^{3+}.

higher charge states. Small number of dressing electrons causes this domination of Coulomb interaction over the short range potential and hence more or less Rutherford behavior is observed in elastic DCS. Some hints of structure is observed for backward scattering for N^{7+} particularly in figure 3(c). Perhaps, this is due to use of Fermi distribution of nuclear charge instead of the point charge. Fading of interference structure occurs due to the increase of charge states at a specific energy and the increase of energy at a particular charge state. Former causes the increasing domination of

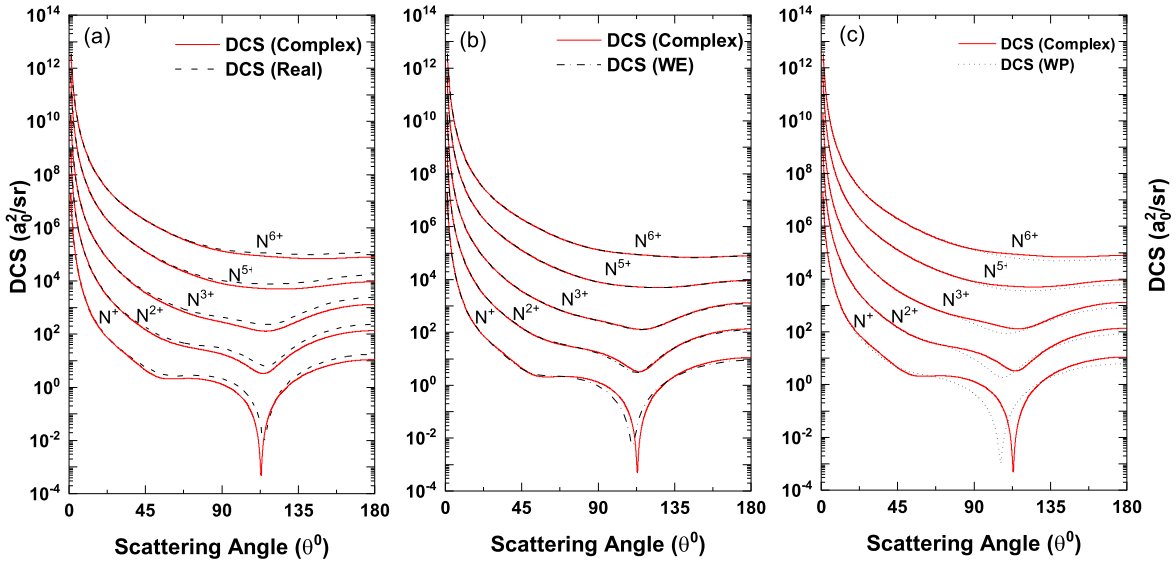

Figure 6. Effects of (a) absorption, (b) exchange and (c) polarization potential on elastic DCS (a_0^2/sr) for the scattering of electron from N^+ ($\times 10^0$), N^{2+} ($\times 10^1$), N^{3+} ($\times 10^2$), N^{5+} ($\times 10^3$) and N^{6+} ($\times 10^4$) at $E_i = 20$ eV. Theoretical: Present work (solid, dash, dash dot and short dot lines). WE in figure (b) stands for potential without exchange and WP in figure (c) stands for potential without polarization.

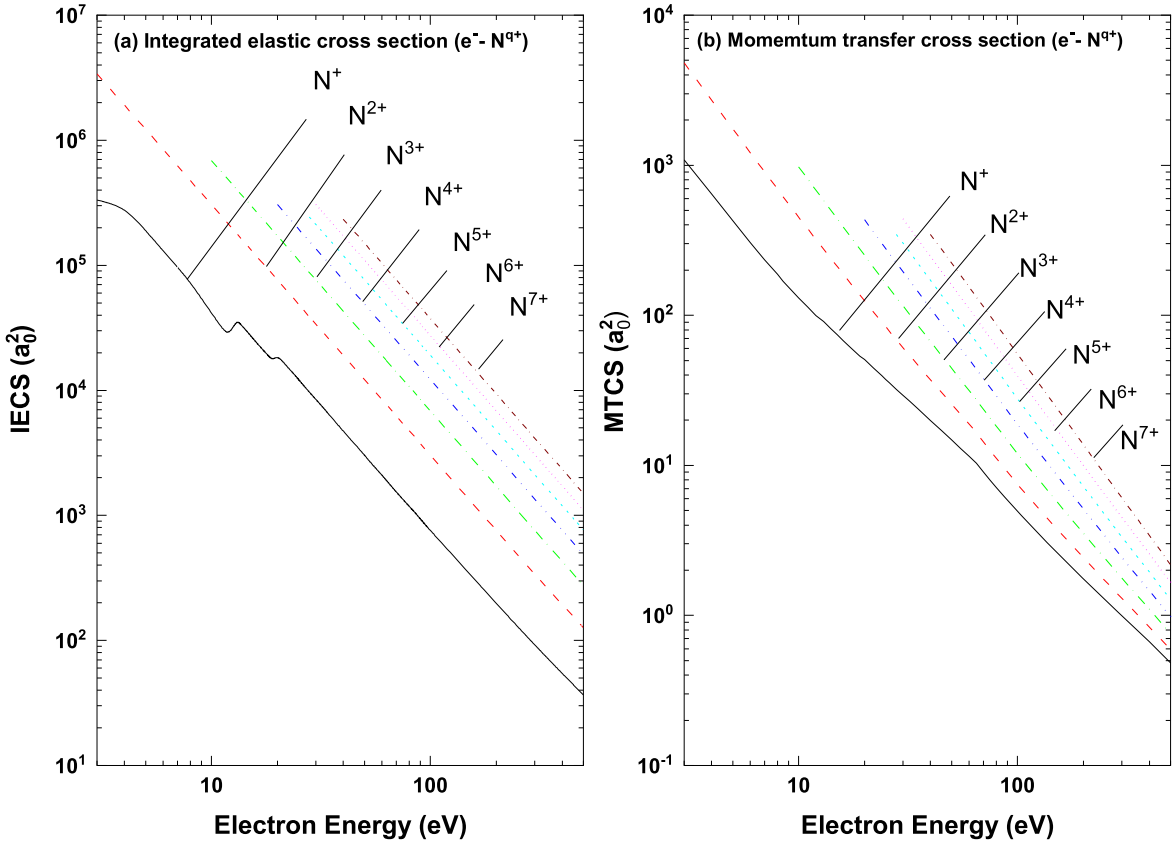

Figure 7. (a) IECS (a_0^2) and (b) MTCS (a_0^2) for the elastic scattering of electrons from N^+ - N^{7+} as a function of incident energy.

Coulomb potential and the latter causes the incoherent interference of large number of angular momentum waves. This dwindling of interference structure throughout the ionic series and considered energy range is illustrated in figures 4 and 5. From figures 1–5, it is observed that glory maximum [32] for backscattering, caused by the screening of nuclear Coulomb potential by atomic electrons, is noticeable for ions of lower degrees of ionicities and at low incident energies.

In figure 6, we present the effects of absorption, exchange and polarization on elastic DCSs. The effects of absorption is noticed throughout the series following a decline of elastic DCS at intermediate and large angles. From

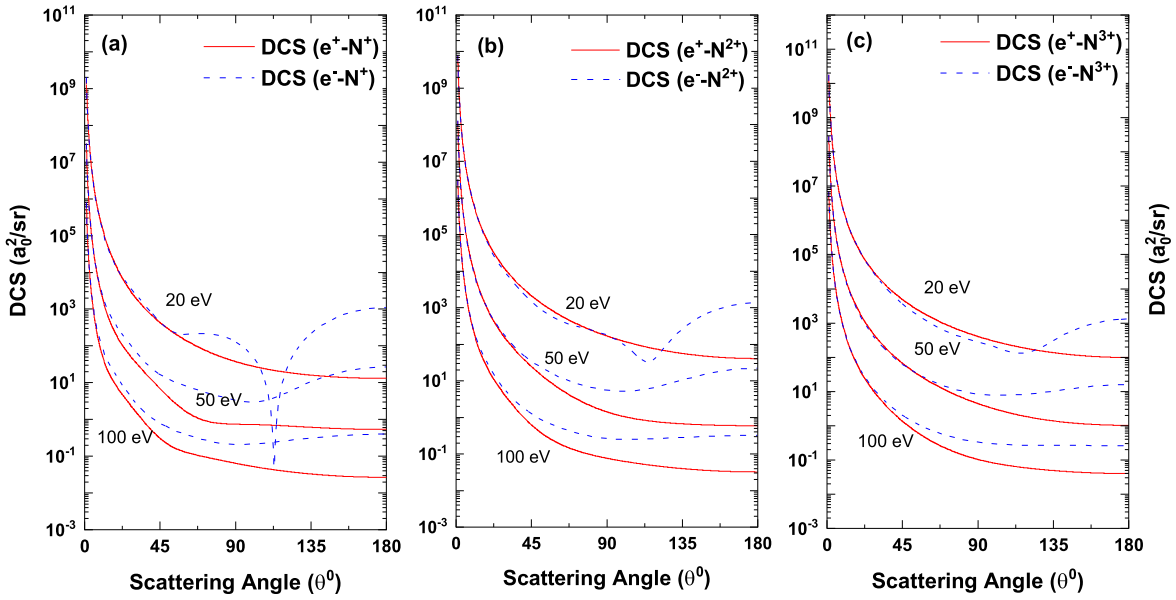

Figure 8. DCS (a_0^2/sr) for the scattering of electrons and positrons from (a) N^+, (b) N^{2+} and (c) N^{3+} at $E_i = 20$ eV ($\times 10^2$), 50 eV ($\times 10^1$) and 100 eV ($\times 10^0$). Theoretical: Present work (solid and dash lines).

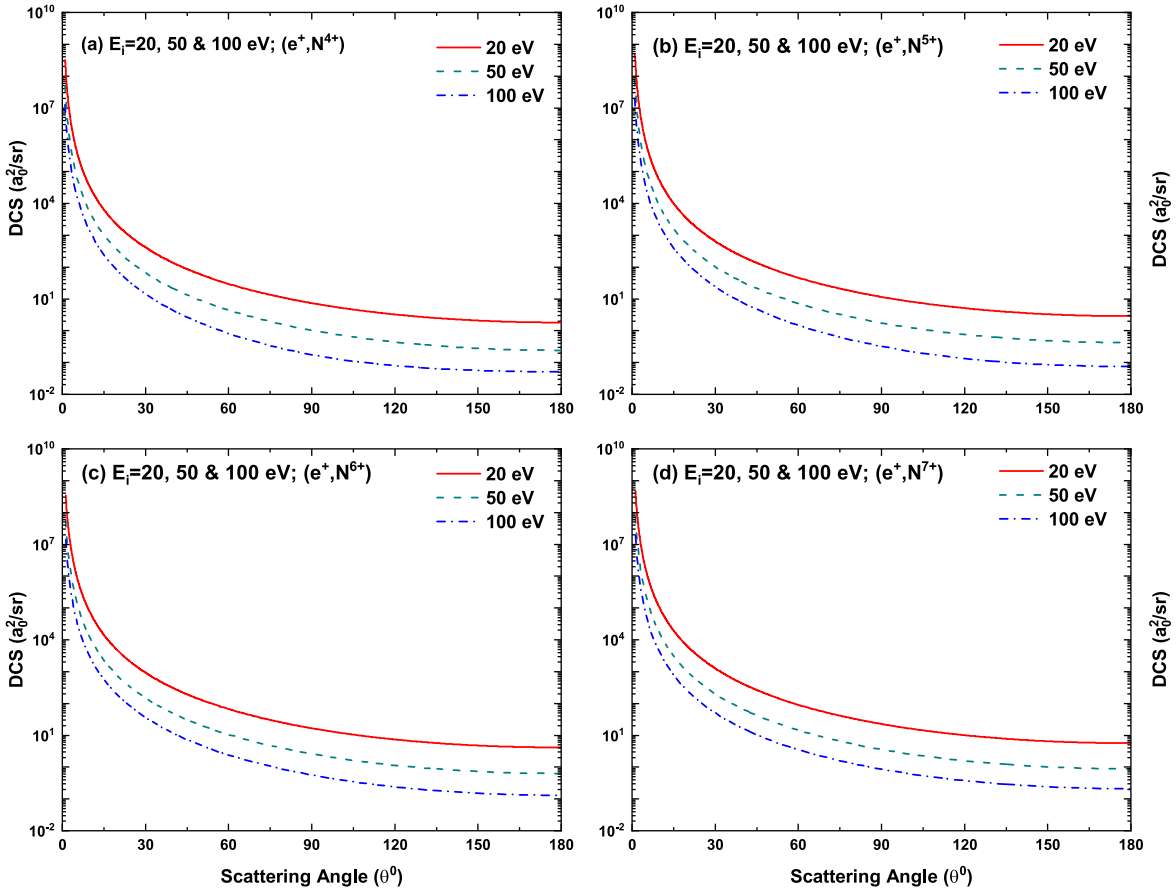

Figure 9. DCS (a_0^2/sr) for the scattering of positrons from (a) N^{4+}, (b) N^{5+}, (c) N^{6+} and (d) N^{7+} at $E_i = 20$ eV, 50 eV and 100 eV. Theoretical: Present work (solid, dash and dash dot lines).

figure 6(b), it is evident that inclusion of exchange potential causes a rise in elastic DCS for backward scattering. The effect is insignificant for forward scattering. This is because exchange can take place significantly when the projectile electron penetrates the ionic core. Rearrangement collision is significant for low charge state as there are more dressing electrons to exchange for. For the same reason, exchange decreases as the stripping increases. It is noticed from

figure 6(c) that polarization potential plays significant role throughout the series. Inclusion of polarization causes a rise in DCS and a shifting of interference minimum towards right. In figure 7, we present IECS and MTCS for the elastic scattering electrons by the ions of nitrogen isonuclear series. A rise in cross section is espied with the increase of ionicity. Diminution of screening effect with the increase of ionicity causes this increase but at the same time this diminution helps the nuclear potential to dominate over the screening and hence slow down this rise of cross sections.

In figure 8, we present the scattering of positron from N^{+}, N^{2+} and N^{3+} at 20, 50 and 100 eV and compare with the corresponding electron-ion scattering. Interference effect and glory maximum for backscattering [32] are observed in DCS for electron scattering but more or less Rutherford scattering is observed for positron scattering. In case of electron-ion scattering short range and long range potentials act as coherent sources while repulsive potential of the ion in case of positron scattering prevents the generation of such coherent sources. We present DCS for the elastic collisions of positrons from N^{4+}. N^{5+}, N^{6+} and N^{7+} at 20, 50 and 100 eV in figure 9. Similar aforesaid trend is observed in these DCSs.

4. Conclusion

In this work, we investigate the elastic scattering of electrons and positrons from the ions of nitrogen isonuclear series. To carry out this investigation, we calculate DCS, IECS and MTCS over the energy range 1–500 eV within Dirac partial wave analysis employing a modified Coulomb potential. We choose such an energy range for the isonuclear series so that it can cover the variation of interference structure with respect to energy. Interference structure is prominently observed for the elastic collisions of low energy electrons from the ions of lower degree of ionicity. This interference is due to the coherent superposition of the waves scattered from short range and asymptotic Coulomb potentials. Low projectile velocity causes enhanced electron-electron correlation and thereby makes the short range potential prominent contributor to the sharp structure observed in elastic DCS. Both increasing charge states and increasing energy weaken the interference structure. Former is due to the domination of Coulomb potential following the diminution of the screening effect and the latter is due to the incoherent interference of large number of angular momentum waves. Glory maximum for backscattering [32] is observed noticeably for low incident energies and lower degrees of ionicities. Effect of absorption throughout the series is observed prominently following a drop in elastic DCS at intermediate and high energies. Exchange potential excercises its effect on scattering for lower degrees of ionicities. It increases DCS for backward scattering. Polarization potential plays significant role throughout the series. Inclusion of this potential causes a rise in elastic DCS and a shift of interference minimum. IECS and MTCS show monotonic behavior over the energies investigated herein. An increase in these cross sections is noticed with the increase of charge states. It is noticed that the aforesaid increase occurs slowly with the increase of ionicity. More or less Rutherford like behavior is observed for positron scattering from nitrogen ions due to the Coulomb repulsion. More data, theoretical or experimental, are needed to validate our theoretical findings and refinement of the theory. Results of our calculations might be helpful to other theoretical or experimental works for comparison and applications.

ORCID iDs

M Shorifuddoza https://orcid.org/0000-0003-1904-4604
Mahmudul H Khandker https://orcid.org/0000-0001-9097-923X
A K F Haque https://orcid.org/0000-0002-1735-3967
M Alfaz Uddin https://orcid.org/0000-0003-3911-0074

References

[1] Khandker M H, Haque A K F, Maaza M and Uddin M A 2019 Elastic scattering of electrons from the ions of argon isonuclear series *Phys. Scr.* **94** 075402
[2] Brotton S J, McKenna P, Gribakin G and Williams I D 2002 Angular distribution for the elastic scattering of electrons from Ar^{+} ($3s^{2}3p^{5}\ ^{2}p$)above the first inelastic threshold *Phys. Rev.* A **66** 062706
[3] Gao X and Li J-M 2014 Precision spectroscopy and electron-ion scattering *Phys. Rev.* A **89** 022710
[4] Müller A 1996 Fundamentals of electron-ion interaction *Hyperfine Interact.* **99** 31–45
[5] Khandker M H, Haque A K F, Maaza M and Uddin M A 2020 Scattering of $e^{\pm}$ from the neon isonuclear series over the energy range 1 eV–0.5 Gev *Japan. J. Appl. Phys.* **59** SHHA05
[6] Jean P, Gillard W, Marcowith A and Ferrière K 2009 Positron transport in the interstellar medium *Astronomy & Astrophysics* **508** 1099–116
[7] Chappell C R, Olsen R C, Green J L, Johnson J F E and Waite J H 1982 The discovery of nitrogen ions in the Earth's magnetosphere *Geophys. Res. Lett.* **9** 937–40
[8] Smith H T, Shappirio M, Sittler E C, Reisenfeld D, Johnson R E, Baragiola R A, Crary F J, McComas D J and Young D T 2005 Discovery of nitrogen in Saturn's inner magnetosphere *Geophys. Res. Lett.* **32**
[9] McElroy M B 1967 Atomic nitrogen ions in the upper atmosphere *Planet. Space Sci.* **15** 457–62
[10] Collins C B, Carroll J M and Taylor K N 1978 Gain and saturation of the nitrogen ion laser *Appl. Phys. Lett.* **33** 175–7
[11] Walther S R, Leung K N and Kunkel W B 1990 Production of atomic nitrogen ion beams *Rev. Sci. Instrum.* **61** 315–7
[12] Schmidt M E, Akabori M and Mizuta H 2018 *Nitrogen ion microscopy. In Ion Beam Applications* (Rijeka: InTech)
[13] Ramsauer C 1921 Über den wirkungsquerschnitt der gasmoleküle gegenüber langsamen elektronen *Ann. Phys.* **369** 513–40
[14] Townsend J S and Bailey V A 1922 LXX. The motion of electrons in argon *The London, Edinburgh, and Dublin Philosophical Magazine and Journal of Science* **43** 593–600
[15] Costello D G, Groce D E, Herring D F and McGowan J W 1972 (e^{+}, He) Total Scattering *Can. J. Phys.* **50** 23–33
[16] Williams I D, Srigengan B, Greenwood J B, Newell W R, Platzer A and O'Hagan L 1997 Elastic scattering of electrons from multiply charged ions *Phys. Scr.* **T73** 119–20

[17] Huber B A, Ristori C and Kuüchler D 1993 Differential electron scattering by multiply charged ions *AIP Conf. Proc.* 274 *(Manhattan, Kansas (USA), 28 Sep − 2 Oct 1992)* pp 455–62
[18] Szydlik P P, Kutcher G J and Green A E S 1974 Independent-particle-model study of the elastic scattering of low-energy electrons by positive ions *Phys. Rev.* A **10** 1623–32
[19] Shepherd J T and Dickinson A S 1999 Elastic scattering of electrons from positive ions *J. Phys. B: At. Mol. Opt. Phys.* **32** 513–25
[20] McCarroll R and Valiron P 1979 Charge exchange of N^{3+} ion with atomic hydrogen in the intersteller gas *Astron. Astrophys.* **78** 177–80
[21] Greenwood J B and Williams I D 1997 Elastic scattering of electrons from highly charged ions in plasmas *Phys. Scr.* **T73** 108–9
[22] Novikov S A, Bromley M W J and Mitroy J 2004 Positron scattering and annihilation from hydrogenlike ions *Phys. Rev.* A **69** 052702
[23] Hahn B, Ravenhall D G and Hofstadter R 1956 High-energy electron scattering and the charge distributions of selected nuclei *Phys. Rev.* **101** 1131–42
[24] Desclaux J P 1975 A multiconfiguration relativistic DIRAC-FOCK program *Comput. Phys. Commun.* **9** 31–45
[25] Furness J B and McCarthy I E 1973 Semiphenomenological optical model for electron scattering on atoms *J. Phys. B: At. Mol. Phys.* **6** 2280–91
[26] Salvat F, Jablonski A and Powell C J 2005 ELSEPA—Dirac partial-wave calculation of elastic scattering of electrons and positrons by atoms, positive ions and molecules *Comput. Phys. Commun.* **165** 157–90
[27] Watson K M and Mittleman M H 1960 Effects of the Pauli principle on the scattering of high-energy electrons by atoms *Ann. of Phys.* **10** 268
[28] Salvat F 2003 Optical-model potential for electron and positron elastic scattering by atoms *Phys. Rev.* A **68** 012708
[29] Schiff L I 1968 *Quantum mechanics* (New York: McGraw-Hill)
[30] Rose M E 1961 *Relativistic Electron Theory* (New York: Wiley)
[31] Salvat F, Fernández-Varea J M and Williamson W Jr. 1995 Accurate numerical solution of the radial schrödinger and dirac wave equations *Comput. Phys. Commun.* **90** 151–68
[32] Demkov Y N 1993 Glory effect for the backscattering of negatively charged particles by multicharged ions *AIP Conf. Proc.* 274 (Manhattan, Kansas, USA: American Institute of Physics) pp 512–514